

Shape Coexistence in ^{186}Pb : Beyond-mean-field description by configuration mixing of symmetry restored wave functions

T. Duguet,^{1,*} M. Bender,² P. Bonche,¹ and P.-H. Heenen²

¹Service de Physique Théorique, CEA Saclay, 91191 Gif sur Yvette Cedex, France

²Service de Physique Nucléaire Théorique, Université Libre de Bruxelles, C.P. 229, B-1050 Bruxelles, Belgium

(Dated: December 3 2002)

We study shape coexistence in ^{186}Pb using configuration mixing of angular-momentum and particle-number projected self-consistent mean-field states. The same Skyrme interaction SLy6 is used everywhere in connection with a density-dependent zero-range pairing force. The model predicts coexisting spherical, prolate and oblate 0^+ states at low energy.

PACS numbers: 21.10Dr; 21.10.Pc; 21.60.Jz

The behavior of shell effects away from the valley of stability is a topic of very active investigation, both theoretically and experimentally. For light nuclei, the spherical $N = 20$ and $N = 28$ shells disappear in neutron-rich isotopes, leading to strongly deformed ground states and large $B(E2)$ transition probabilities between the first 2^+ state and the ground state [1]. In contrast, the magic proton number $Z = 82$ is particularly strong and its influence persists even in very neutron-deficient nuclei. The ground state of Pb isotopes is known to be spherical down to ^{182}Pb [2]. The weakening of magicity of the $Z = 82$ shell manifests itself by the appearance of low-lying 0^+ states [3]. At least one low-lying excited 0^+ state has been observed in all even-even Pb isotopes between ^{182}Pb and ^{194}Pb at excitation energies below 1 MeV, the most extreme cases being ^{188}Pb and ^{186}Pb [4, 5] with two excited 0^+ states below 700 keV.

Two different kinds of models have been invoked to explain the coexistence of several 0^+ states at low energy [6]. In a shell model picture [5], the first excited 0^+ state observed from ^{202}Pb down to ^{186}Pb is interpreted as a two-quasiparticle proton configuration $(\pi h9/2)^2$ while the second one in ^{188}Pb and ^{186}Pb and also the first one in ^{184}Pb as a four-quasiparticle configuration $(\pi h9/2)^4$. In this picture, neutrons and protons outside the inert core interact through pairing and quadrupole interactions to generate deformed structures. Such a model requires to drastically truncate the configuration space. Up to now, it has been only applied in a very schematic qualitative way.

In mean-field models, the 0^+ states observed at low energies are associated with coexisting energy minima which appear for different values of the axial quadrupole moment [7]. The ground state corresponds to the spherical minimum and the excited 0^+ to deformed states with an oblate (in the heaviest Pb isotopes) or a prolate (in ^{184}Pb up to ^{188}Pb) shape.

However, shape coexistence in the neutron-deficient Pb region cannot be described on the level of mean-field models in a fully satisfactory way. The minima obtained as a function of the quadrupole moment are rather shal-

low and dynamical effects such as quadrupole vibrations may affect the very existence of these minima. Tajima *et al.* [8] and more recently Chasman *et al.* [9] have studied the quadrupole dynamics of Pb isotopes by performing a configuration mixing of mean-field states with different axial quadrupole moment. Their results support the interpretation of the deformed minima as excited 0^+ states: the lowest excited states obtained in the configuration mixing calculation have average deformations close to that of the mean-field minima. However, the calculated excitation energies overestimate the experimental values. Diabatic effects have been studied by Tajima *et al.* who have included for each axial quadrupole moment the lowest Hartree-Fock+BCS (HFBCS) configuration and the two-quasiparticle deformed proton configurations $(\pi h9/2)^2$. Tajima *et al.* have shown that these configurations do not influence significantly the configuration-mixing results and that they can be neglected.

The experimental data on neutron deficient Pb isotopes are not limited to a few 0^+ states. Rotational bands have also been observed whose properties have served to interpret the excited 0^+ as of oblate and prolate deformations. Transition probabilities between the states are also known in some cases. It seems therefore highly desirable to apply to Pb isotopes the configuration-mixing method that we have recently developed [10], which permits to treat simultaneously the most important symmetry restorations and the mixing with respect to a collective variable. We present here an application to ^{186}Pb . This isotope has the unique property to have 0^+ states as its lowest three states, with the excitation energy of the second and third 0^+ being minimal among the known Pb isotopes [5]. While the ground state is assumed to be spherical, the 0^+ states observed at 532 keV and 650 keV are interpreted as oblate and prolate configurations.

The “projected” configuration mixing of mean-field wave functions as performed here has several goals. The particle-number projection removes unwanted contributions coming from states with different particle numbers, which are an artifact of the BCS approach. The angular momentum projection separates the contribution from

different angular momenta to the mean-field states and generates wave functions in the laboratory frame with good angular momentum. Finally, the variational configuration mixing with respect to a collective coordinate, the axial quadrupole moment in this work, removes the contributions to the ground state coming from collective vibrations and simultaneously provides the excitation spectrum corresponding to this mode.

The starting point of our method is a set of independent HFBCS wave functions $|q\rangle$ generated by mean-field calculations with a constraint on a collective coordinate q . Such mean-field states break several symmetries of the exact many-body states. Wave functions with good angular momentum and particle numbers are obtained by the restoration of rotational and particle-number symmetry on $|q\rangle$:

$$|JMq\rangle = \frac{1}{\mathcal{N}} \sum_K g_K^J \hat{P}_{MK}^J \hat{P}_Z \hat{P}_N |q\rangle, \quad (1)$$

where \mathcal{N} is a normalization factor. \hat{P}_{MK}^J , \hat{P}_N , \hat{P}_Z are projectors onto angular momentum J with projection M along the laboratory z-axis, neutron number N and proton number Z respectively. We impose axial symmetry and time reversal invariance and therefore, K can only be 0 and we shall omit the coefficient $g_K^J = \delta_{K0}$. This excludes the description of γ bands with $K = 2$ from our model.

A variational configuration mixing on the collective variable q is then performed for each angular momentum

$$|JMK\rangle = \sum_q f_k^{JM}(q) |JMq\rangle. \quad (2)$$

The weight functions $f_k^{JM}(q)$ are determined by requiring that the expectation value of the energy

$$E_k^{JM} = \frac{\langle JMK|\hat{H}|JMK\rangle}{\langle JMK|JMK\rangle}, \quad (3)$$

is stationary with respect to an arbitrary variation $\delta f_k^{JM}(q)$. This prescription leads to the discretized Hill-Wheeler equation [11]. Such a secular problem amounts to a restricted variation after projection in the set of states obtained for different values of the collective variable q . Collective wave functions $g_k^{JM}(q)$ in the basis of the intrinsic states are then obtained from the set of weight functions $f_k^{JM}(q)$ by a basis transformation [8]. Since the collective states $|JMK\rangle$ have good angular momentum, quadrupole moments and transition probabilities can be directly determined in the laboratory frame of reference without further approximations and using the bare proton charge.

The same effective interaction is used to generate the mean-field wave functions and for the configuration mixing calculation. We have chosen the Skyrme interaction SLy6 in the mean-field channel [12] and a density-dependent zero-range force as defined in [13] in the pairing channel. The pairing equations are solved using

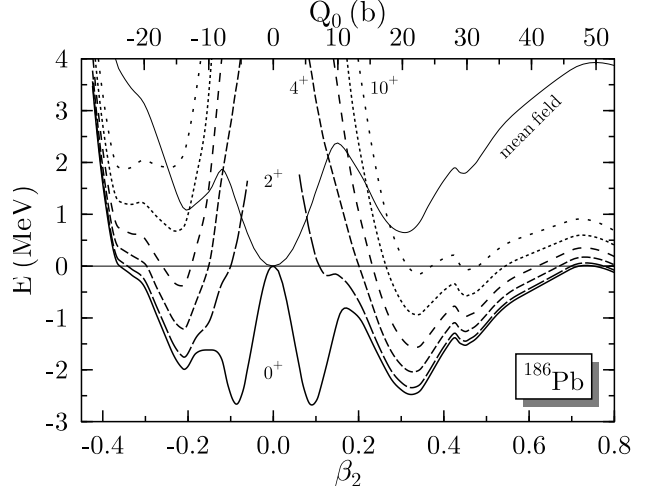


FIG. 1: Particle-number projected (“mean field”) and particle-number and angular-momentum projected potential energy curves up to $J = 10 \hbar$ for ^{186}Pb as a function of the mass quadrupole moment in barn (upper axis) or equivalently in terms of β_2 (lower axis). The energy reference is that of the projected spherical mean-field state.

the Lipkin-Nogami prescription, as done in [10]. The two-body center-of-mass correction is self-consistently included in the interaction SLy6 [12], however, in the present calculations, it is included *a posteriori* at the mean-field level and in the projection and configuration-mixing calculations.

On figure 1 is plotted the deformation energy of ^{186}Pb before and after projection on angular momentum. All curves are drawn versus the intrinsic axial quadrupole moment of the unprojected mean-field states. As projected $J = 0$ states are spherical, this “quadrupole moment” is only a convenient way to label the projected states. The curve labeled “mean-field” plots the deformation energy after particle-number projection only. It exhibits a spherical global minimum as well as local minima at prolate and oblate deformations. While the deformation energy of the prolate minimum fortuitously reproduces the experimental value of 0.650 MeV for the prolate 0^+ state, the 1.1 MeV deformation energy of the oblate minimum overestimates the experimental value of 0.532 MeV for the oblate 0^+ state. A fourth very shallow minimum can be seen at a deformation β_2 around 0.5; it is too shallow to be safely associated with a physical state.

The energy curves obtained after angular momentum projection are also shown on figure 1. At moderate deformations around the prolate and oblate minima, the mean-field states are dominated by angular-momentum components with $J \geq 8 \hbar$, which is reflected by the fact that all projected energy curves are far below the mean-field curve. The spherical mean-field state is rotationally invariant and therefore contributes to $J = 0$ only. Two

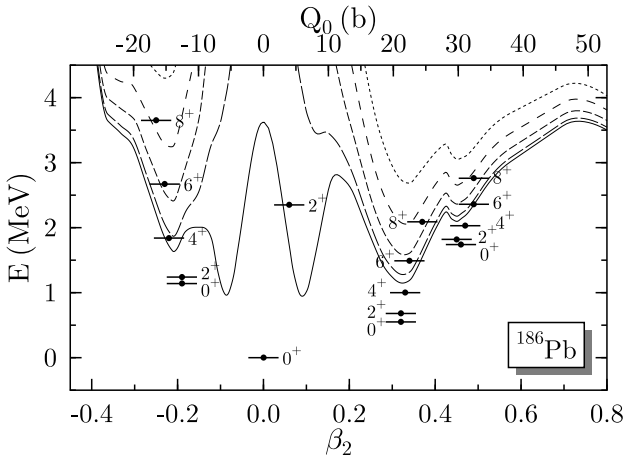


FIG. 2: Spectrum of the lowest positive parity bands with even angular momentum and $K = 0$, as a function of the deformation (see text). The angular momentum projected energy curves are shown for comparison. The energy reference is that of the calculated 0^+_1 ground state.

minima appear at small deformations around $\beta_2 = \pm 0.1$. They do not correspond to two different states, but to the correlated spherical state (see below). For larger prolate and oblate deformations, the energy difference between the mean-field and $J = 0$ curves stays nearly constant. The prolate and oblate mean-field minima are present in all the projected energy curves. Angular momentum projection reduces the energy difference between the spherical ($|\beta_2| \approx 0.1$) and deformed minima to 0.2 MeV for the prolate and 0.68 MeV for the oblate well. While the prolate potential well is pronounced for all angular momenta, the oblate well is now very shallow for $J = 0$.

The excitation energies E_k^{JM} of the collective states $|JMK\rangle$ obtained from the configuration mixing calculation are shown in figure 2. Each of these states is represented by a bar drawn at the average intrinsic deformation $\sum_q \beta_2(q) |g_k^{JM}(q)|^2$, where $\beta_2(q)$ is the deformation of the mean-field state. The excitation spectrum is divided into bands corresponding to different deformations. Configuration mixing lowers the energy of the lowest collective states with respect to the projected energy curves. The energy gain is the largest for the ground state, increasing the excitation energies of the prolate and oblate 0^+ states.

The corresponding collective wave functions $g_k^{JM}(q)$ are plotted in figure 3. Their square gives the weight of each mean-field state $|q\rangle$ in the collective state $|JMK\rangle$.

The ground state wave-function is spread in a similar way on both oblate and prolate sides with a zero average β_2 deformation. The wave functions of the first two excited 0^+ states are strongly peaked at either prolate (0^+_2) or oblate deformations (0^+_3), with their tails extending into the spherical well. For higher J values, the shape of the wave functions confirms their assignment to oblate

and prolate bands as already hinted in figure 2. As there is no spherical well for $J > 0$ states, their wave functions mix only prolate and oblate configurations. Starting with $J = 4 \hbar$, states are strongly localized and are predominantly either prolate or oblate. The shapes of the 0^+_4 , 2^+_3 , and 4^+_3 wave functions suggests their interpretation as a rotational band built onto a β vibration within the prolate well, while the wave function of the 2^+_4 state indicates that it corresponds to a vibrational state, which is spread over the whole potential well.

The calculated spectrum is compared to the experimental data in figure 4. The energy of the prolate 0^+ state at 0.55 MeV is very close to the experimental energy contrary to the excitation energy of the oblate 0^+ state which is largely overestimated. The experimental data even suggest that the oblate state is slightly below the prolate one. A nice result is that the structure of the first three 0^+ states are dominated by spherical, prolate and oblate configurations respectively and supports the interpretation of the experimental data as evidence for shape coexistence. This could not have been guessed from the deformation energy curves (see figure 1) where the oblate well has a depth of only 500 keV and the prolate one of 1 MeV. The excitation energies of the first two excited 0^+ states are even quite close to the energy differences between the deformed minima and the spherical minimum of the mean-field deformation energy curve.

The energies of the low-lying states in all bands are

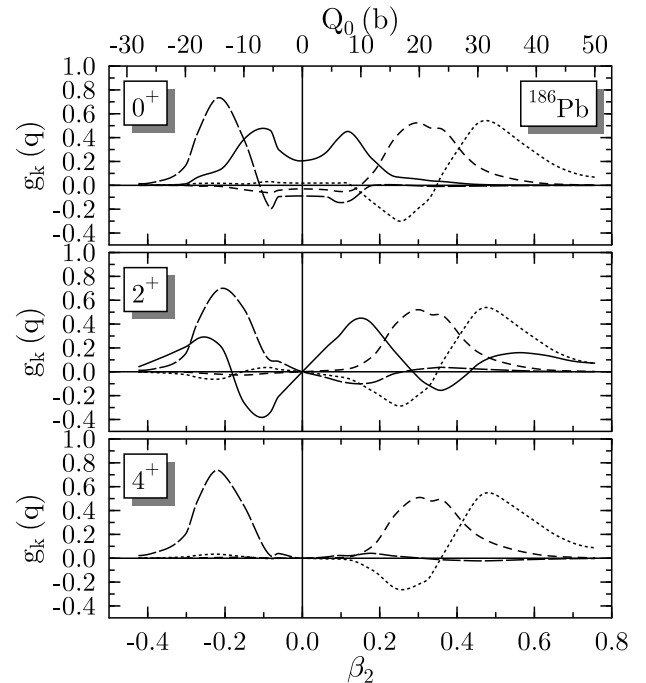


FIG. 3: GCM wave functions $|Jk\rangle = \sum_q g_k(q)|Jq\rangle$ of the lowest states. Solid lines denote spherical, long-dashed lines oblate, dashed lines prolate, and dotted lines the β band in the prolate well.

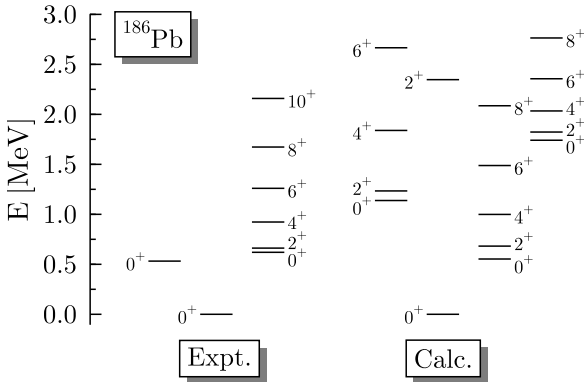


FIG. 4: Comparison between the calculated excitation energies and the available experimental data for low-lying states in ^{186}Pb . From the left to the right the spectra show oblate, spherical and prolate bands.

perturbed from a rotational behavior by the configuration mixing, the $E_{0^+} - E_{2^+}$ energy difference of the prolate and oblate bands being lower than expected from the $E_{2^+} - E_{4^+}$ spacing. This is a consequence of the stronger mixing of states for $J = 0$ than for higher J values. For the prolate band, however, the calculated perturbation is smaller than in experiment, probably a consequence of the overestimated energy of the oblate band head which decreases the mixing between the deformed configurations.

Calculated transition probabilities for $J > 2$ states confirm the separation of the excited states into rotational bands with very small $B(E2)$ transitions between bands. While the transition quadrupole moments Q_0 of the oblate ($Q_0 \approx -600 \text{ e fm}^2$ or $\beta_2 \approx -0.2$) and prolate ($Q_0 \approx 1000 \text{ e fm}^2$ or $\beta_2 \approx 0.34$) bands slowly grow with angular momentum, the deformation of the third rotational band stays nearly constant at about $Q_0 \approx 1400 \text{ e fm}^2$ ($\beta_2 \approx 0.49$), in agreement with the systematics of the minima in the projected energy curves in figure 1. The $B(E2)$ values for the in and out of bands $2^+ \rightarrow 0^+$ transitions confirm that the low-lying 0^+ states are mixed.

Our results strongly support the interpretation of the Pb isotopes spectra as an evidence for shape coexistence. There remains, however, a significant over-estimation of one of the band's excitation energy, which can be due to several ingredients of the model:

- the effective mean-field interaction. Small differences between interactions (surface tension, spin-orbit strength, ...) shift the relative energies of the various coexisting minima at the mean-field level [14, 15]. In a calculation with the Skyrme SLy4 interaction, the prolate and oblate 0^+ states are pushed up to 1.05 MeV and 1.39 MeV respectively, as can be expected from the overall stiffer energy surface of that interaction [16].

- the strength and the form factor of the pairing interaction. A test with a reduced pairing strength (-1100

MeV fm 3) shows that the energies of the prolate and oblate minima of the deformation energy curves are reduced to 0.2 MeV and 0.65 MeV respectively.

- the configuration space used in the configuration mixing. To test this possible source of error, we have enlarged the space by including the oblate $(\pi h9/2)^2$ two-quasiparticle proton configurations, as was done by Tajima *et al.* [8]. As in this paper, the results are changed by at most 100 keV.

- the inclusion of triaxial quadrupole configurations. Projection on J becomes much heavier numerically, and this is still beyond present numerical possibilities.

- generalized interaction for calculations beyond mean field. Most mean-field interactions depend on the one-body density. It is known since the 70s that this density dependence can have two different origins: either a three-body force or a resummation of (short-range) correlations beyond mean field. To generalize this dependence for the non-diagonal matrix elements appearing beyond the mean-field approximation we have chosen the generalisation stemming from a three-body interaction. Duguet and Bonche [17] have shown that resummation of correlations beyond mean-field gives rise to another generalisation of the Skyrme force. The study of shape coexistence in nuclei like the Pb isotopes could be a good place to determine the merits of both generalisations of the Skyrme force.

This research was supported in part by the PAI-P5-07 of the Belgian Office for Scientific Policy. We thank M. Huyse, R. V. F. Janssens, and P. Van Duppen for fruitful and inspiring discussions. M. B. acknowledges support through a European Community Marie Curie Fellowship.

* Current address:Argonne National Laboratory, Physics Division, Argonne, IL 60439

- [1] P.-G. Reinhard *et al.*, Phys. Rev. C **60**, 014316 (1999).
- [2] J. Wauters *et al.*, Phys. Rev. C **50**, 2768 (1994).
- [3] R. Julin *et al.*, J. Phys G **27**, R109 (2001).
- [4] J. Heese *et al.*, Phys. Lett. **B302**, 390 (1993).
- [5] A. N. Andreyev *et al.*, Nature **405**, 430 (2000).
- [6] J. L. Wood *et al.*, Phys. Rep. **215**, 101 (1992).
- [7] W. Nazarewicz, Phys. Lett. **B305**, 195 (1993).
- [8] N. Tajima *et al.*, Nucl. Phys. **A551** (1993) 409.
- [9] R. R. Chasman *et al.*, Phys. Lett. **B513**, 325 (2001).
- [10] A. Valor *et al.*, Nucl. Phys. **A671**, 145 (2001).
- [11] D. L. Hill and J. A. Wheeler, Phys. Rev. **89**, 1102 (1953).
- [12] E. Chabanat *et al.*, Nucl. Phys. **A635**, 231 (1998).
- [13] C. Rigolet *et al.*, Phys. Rev. C **59**, 3120 (1999).
- [14] M. Bender *et al.*, Eur. Phys. J. **A14**, 23 (2002).
- [15] T. Niksic *et al.*, Phys. Rev. C **65**, 054320 (2002).
- [16] M. Bender *et al.*, Eur. Phys. J. **A7**, 467 (2000).
- [17] T. Duguet and P. Bonche, preprint nucl-th/0210057.